



Screening of immune-related biological markers for aneurysmal subarachnoid hemorrhage based on machine learning approaches

Jing Liu^{a,1}, Zhen Sun^{b,1}, Yiyu Hong^a, Yibo Zhao^a, Shuo Wang^a, Bin Liu^{a,**}, Yantao Zheng^{a,*}

^a Department of Emergency, Zhujiang Hospital, Southern Medical University, China

^b Nanyang Central Hospital, China

ARTICLE INFO

Keywords:

Aneurysmal subarachnoid hemorrhage
Bioinformatics analysis
Immune infiltration
Weighted gene co-expression network analysis

ABSTRACT

Background: Aneurysmal subarachnoid hemorrhage (aSAH) is a common hemorrhagic condition frequently encountered in the emergency department, which is characterized by high mortality and disability rates. However, the precise molecular mechanisms underlying the rupture of an aneurysm are still not fully understood. The primary objective of this study is to elucidate the fundamental molecular mechanisms underlying aSAH and provide novel therapeutic targets for the treatment of aSAH.

Methods: The gene expression matrix of aSAH was downloaded from the Gene Expression Omnibus (GEO) database. In this study, we employed weighted gene co-expression network analysis (WGCNA) and differential gene expression analysis (DEGs) screening to identify crucial modules and genes associated with aSAH. Furthermore, the evaluation of immune cell infiltration was conducted through the utilization of the single-sample gene set enrichment analysis (ssGSEA) technique and the CIBERSORT algorithm. The study utilized Gene Set Variation Analysis (GSVA), Gene Ontology (GO), and Kyoto Encyclopedia of Genes and Genomes (KEGG) to investigate and comprehend the fundamental biological pathways and mechanisms.

Results: Using WGCNA, six gene co-expression modules were constructed. Among the identified modules, the yellow module, which encompasses 184 genes, demonstrated the most significant correlation with aSAH. Consequently, it was determined to be the central module responsible for governing the pathogenesis of aSAH. Additionally, the application of WGCNA, LASSO regression, and multiple factor logistic regression analysis revealed ARHGAP26 and SLMAP as the key genes associated with aSAH. Furthermore, the diagnostic efficacy of these pivotal genes in aSAH was confirmed through the use of receiver operating characteristic (ROC) curve analysis, validating their discriminative potential. Moreover, the utilization of GO and KEGG pathway analysis revealed a significant enrichment of inflammation-related signaling in aSAH.

Conclusion: The genes ARHGAP26 and SLMAP were identified as significant predictors of aSAH. Accordingly, these genes demonstrate significant potential to function as novel biological markers and therapeutic targets for aSAH.

1. Introduction

Subarachnoid hemorrhage (SAH) refers to a collection of clinical symptoms that result from the extravasation of blood into the subarachnoid space due to the rupture of cerebral vasculature, precipitated by diverse etiologies. This particular condition is a widely observed and crucial medical emergency that carries substantial implications for the outcomes of patients. The occurrence of SAH varies by region and ethnicity. Based on existing literature, it has been reported that the

annual incidence of SAH ranges from 1 to 27 cases per 100,000 individuals [1,2]. In addition, its incidence accounts for 5–10 % of all strokes [1,2]. SAH is a destructive subtype of stroke, with the majority of cases being attributed to the rupture of intracranial aneurysms (IAs), aneurysmal subarachnoid hemorrhage (aSAH) results in various physiological consequences, including elevated intracranial pressure, reduced cerebral blood flow, and diminished cerebral perfusion pressure [3]. aSAH is associated with a considerable mortality and disability rate, as evidenced by an estimated 46 % of individuals who survive the

* Corresponding author.

** Corresponding author.

E-mail addresses: nysylb@163.com (B. Liu), 51983782@qq.com (Y. Zheng).

¹ Jing Liu and Zhen Sun are co-first authors.

condition encountering irreversible neurological impairment [4].

The pathogenesis of aneurysmal subarachnoid hemorrhage (aSAH) is a multifactorial and intricate process involving several underlying mechanisms. These mechanisms encompass intricate interplays of various factors, including inflammatory responses, aberrant vascular contractility, microthrombus formation, cellular ischemia and hypoxia, brain cell damage, and genetic modulation of gene expression. Perturbations in cerebral arterial hemodynamics can incite endothelial cell inflammation, while a sustained and excessive inflammatory response within the vascular wall can contribute to the development and subsequent rupture of intracranial aneurysms, ultimately leading to subarachnoid hemorrhage [5,6]. The induction of aSAH is facilitated by various cellular components, *viz.* macrophages, lymphocytes, mast cells, and neutrophils, which initiate a series of signal transduction pathways [7]. In recent years, there has been a shift in research emphasis within the field of aneurysms, with a greater focus on investigating the mechanisms underlying the formation of intracranial aneurysms. Conversely, comparatively less attention has been directed towards studying the subarachnoid hemorrhage resulting from the rupture of aneurysms. Aneurysmal subarachnoid hemorrhage is a perilous condition characterized by a complex pathogenesis that encompasses multiple biological processes. In recent years, increasing number of studies have demonstrated that the immune system plays a significant role in the development and progression of aneurysmal subarachnoid hemorrhage [8]. The use of machine learning approaches for the identification of immune-related biological markers shows great potential as a promising avenue for research. By analyzing data obtained from a large cohort of patients and healthy individuals, immune markers related to aSAH can be identified. Consequently, a predictive model can be established for the early diagnosis and treatment of patients afflicted with aSAH.

The present study reports the screening of intracranial aneurysm rupture-induced subarachnoid hemorrhage dataset in the GEO database. Through the integration of biological information, analytical techniques, and machine learning, we conducted an extensive investigation into the key genes associated with aSAH. This study, therefore, holds significant implications for monitoring the progression of aSAH predicting disease prognosis, and the identification of novel genetic targets for the diagnosis and treatment of aSAH.

2. Materials and methods

2.1. Data collection and preparation

The datasets GSE13353, GSE54083, were obtained from the Gene Expression Omnibus (GEO) database (<http://www.ncbi.nlm.nih.gov/geo>). Detailed specifications and characteristics of the datasets utilized in this study can be found in Table 1, offering comprehensive information on each dataset.

2.2. Differential gene analysis

The merge () function in the R programming language was employed to integrate the GSE13353 and GSE54083 datasets. Ensuring data consistency necessitates the matching of experimental design and sample information. Following this, differential gene screening was conducted using the limma package in the R programming language, which facilitates the computation of P-values and fold changes in gene expression. The screening criteria utilized in this study consisted of logFC >1 and adjusted P-value <0.05. The volcano plot and heat map of differentially

expressed genes were generated using the ggplot2 and Heatmap packages in the R programming language.

2.3. Screening for key modules by weighted gene co-expression network analysis (WGCNA)

The gene co-expression network was constructed using the WGCNA package in the R language. An appropriate soft threshold was selected to ensure that the resulting co-expression network adheres to the properties of a scale-free network. Utilizing the designated soft threshold, the gene co-expression network was established, followed by its analysis through the implementation of the “blockwiseModules” function. Subsequently, the dynamic cut method was employed to partition the modules, and the resulting network was visualized via a hierarchical clustering tree. The WGCNA algorithm was employed to calculate the gene module connectivity and determine the hub genes within each module exhibiting the greatest module connectivity. The modules that exhibited a significant correlation with the phenotype were selected, followed by a screening of the genes within these modules. Subsequently, the identification of the crucial genes associated with the phenotype was conducted. A comprehensive biological annotation and functional analysis of the selected genes was subsequently performed. Through the correlation of gene modules with clinical information on aSAH, this study aimed to ascertain the modules associated with aSAH based on the module-phenotype correlation, and identify the disease-associated genes in these modules.

2.4. Screening of aSAH characteristic genes

The least absolute shrinkage and selection operator (LASSO) regression method was utilized to screen for key genes that were potentially associated with the rupture of aSAH. The data was analyzed using the glmnet package in the R programming language to construct a LASSO regression model. The LASSO regression and cross-validation graphs were subsequently generated, resulting in the identification of the selected feature genes as the output.

2.5. Receiver operating characteristic (ROC) curve analysis

The ROC curve was generated based on the selected gene expression data and the corresponding sample status using the “proc” package within the R software. The weight of each gene was determined using the entropy weighting method, and the ROC curve of four key genes was plotted. The diagnostic efficacy of these four genes for aSAH was assessed by utilizing the area under the receiver operating characteristic curve (AUC). Subsequently, we identified genes that exhibited statistical significance ($P < 0.05$) from a set of highly connected genes (referred to as HUB genes). Additionally, we used a nodal diagram to predict the likelihood of aSAH occurrence.

2.6. Enrichment analysis of GO function, KEGG pathway

Gene enrichment pathway maps were plotted to visually represent the enrichment of differentially expressed genes within biological pathways. The R software (version) was utilized for conducting GO functional analysis, KEGG pathway enrichment analysis, and GSEA. The org.Hs.eg.db package (version) was employed for the purpose of ID conversion. Similarly, the clusterProfiler package (version) was utilized for conducting enrichment analysis. Finally, the ggplot2 package (version) was employed for the purpose of visualization. The selection of the primary enriched functions and pathways of differential genes was based on a threshold of a corrected P-value <0.05 for conducting GO functional analysis and KEGG pathway enrichment analysis.

Table 1

The information of all the datasets in the study.

Datasets	Platform	Treat Case	Sample Size
GSE13353	GPL570	11	19
GSE54083	GPL4133	8	23

2.7. Protein-protein interaction (PPI) network analysis

The utilization of a PPI network can facilitate the identification of hub genes within the differentially expressed genes (DEGs) of aSAH patients. Accordingly, the PPI information of DEGs was obtained from the Search Tool for the Retrieval of Interacting Genes (STRING) database. Subsequently, Cytoscape (v3.7.1) was used for the construction of PPI network.

2.8. Immunoinfiltration analysis

The single-sample gene set enrichment analysis (ssGSEA) method initially assigns ranks to the expression levels of all genes in the sample, thereby determining their relative positions among all genes. Subsequently, the input gene set was queried within the expression data to identify and quantify the presence of corresponding genes, followed by the aggregation of their expression levels. Subsequently, the enrichment score for each gene in the pathway was calculated using the aforementioned values. Additionally, the gene order was shuffled and the enrichment score was recalculated 1000 times. Finally, the integration of the gene set's ultimate enrichment score was achieved by calculating the p-value based on the distribution of gene enrichment scores.

We also used correlation analysis to examine the relationship

between gene expression levels and immune cell content. When the p-value of the correlation test was below 0.05, it indicated the presence of a correlation between the expression of the target gene and the content of immune cells.

Additionally, a heatmap of relative immune cell content was generated to visualize the relative content of each immune cell across various samples. Moreover, by plotting a boxplot of relative immune cell content, we compared the differences in immune cell content across various samples. Finally, we generated a scatter plot of relative immune cell content to visually represent the correlation between immune cell content and phenotype.

3. Result

3.1. WGCNA

The merged dataset was analyzed using the WGCNA network. A suitable soft threshold was selected in order to create a scale-free network, wherein the gene expression patterns above the soft threshold exhibited similarity. The clustering results obtained from the sample in this study demonstrated that by setting the soft threshold to 7, the co-expression network successfully adhered to the principles of scale-free topology, thereby fulfilling the predetermined criteria for the

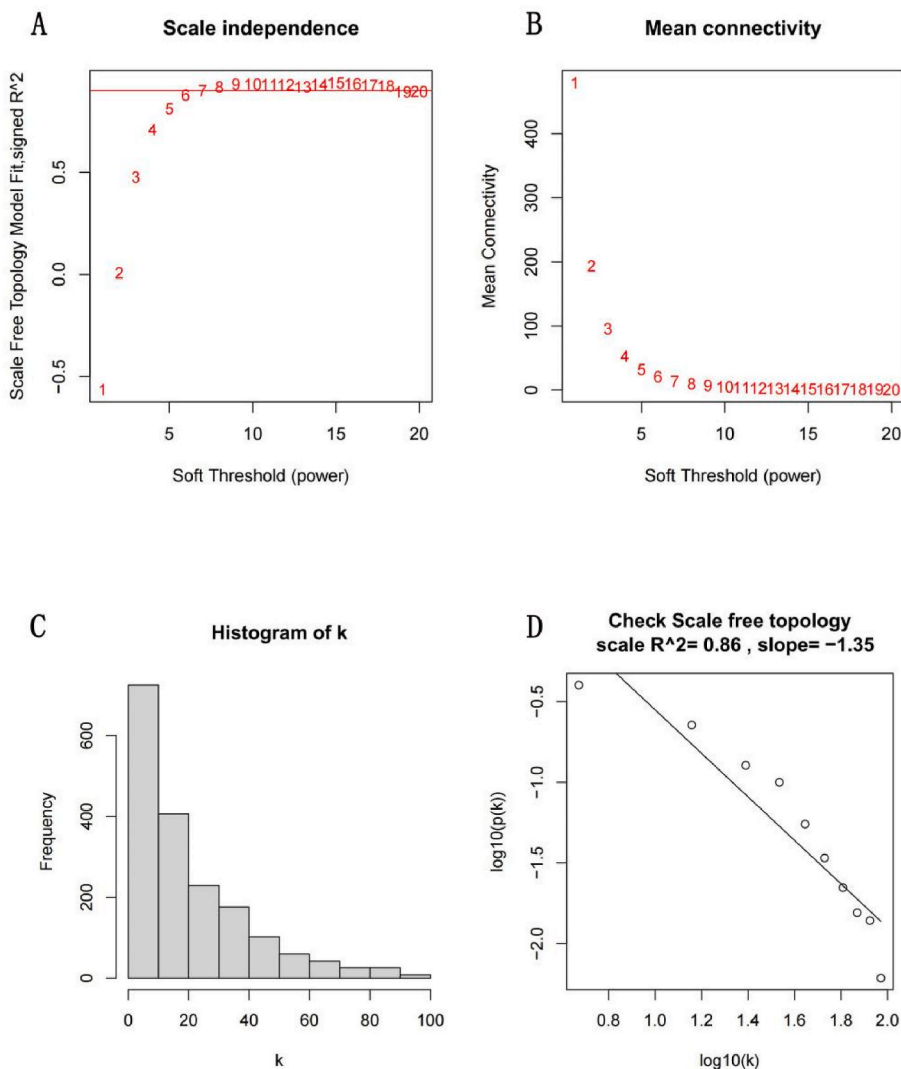


Fig. 1. Soft threshold screening. (A, B) Scale independence and mean connectivity analysis. (C) Histogram of the connectivity distribution. (D) Verification of the scale-free topology.

selected power value (Fig. 1A–D). A hierarchical clustering tree was generated using a power value of 7, resulting in the identification of 6 distinct modules with a merge threshold of 0.25 (Fig. 2A–D). Out of all the modules examined, it was observed that the yellow module, which consisted of 184 genes, exhibited the highest GS. This finding suggests a robust correlation with aSAH along with notable disease progression (Fig. 2D).

3.2. Functional enrichment analysis

The genes within the yellow module were utilized for GO analysis and KEGG pathway enrichment analysis in order to investigate the potential biological processes linked to aSAH. The enrichment analysis conducted for GO-biological processes (GO-BP) revealed a statistically significant enrichment of genes associated with inflammatory responses, among other processes (Fig. 3A). The GO-cellular component (GO-CC) enrichment analysis revealed the participation of genes associated with focal adhesion, cell-substrate junction, and various other cellular components (Fig. 3B). The GO-molecular function (GO-MF) enrichment analysis revealed a notable enrichment of genes associated with insulin-like growth factor binding, extracellular matrix structural constituent, and various other molecular functions (Fig. 3C). The KEGG pathway analysis revealed a notable enrichment of genes associated with the C-type lectin receptor signaling pathway (Fig. 3D).

3.3. Screening key genes

Through the process of gene intersection, a total of 23 genes were identified (Fig. 4A). As a result, 23 genes were obtained for subsequent model building (Fig. 4B). The relative regression coefficients of 23 genes were calculated using LASSO regression analysis. Among them, four

genes, namely ARHGAP26, SLMAP, PCYOX1, and PHF14, were identified as the final selection for establishing the LASSO regression model. These genes demonstrated significant associations with the studied variables and exhibited the strongest predictive power in the model. The LASSO regression path can be observed in Fig. 4C.

3.4. Expression and verification of key genes

In cases of aneurysmal subarachnoid hemorrhage (aSAH), the expression of ARHGAP26 was found to be downregulated, while SLMAP, PCYOX1, and PHF14 showed upregulation. These differential expression patterns exhibited statistical significance, as evidenced by a highly significant *P*-value of < 0.001 (Fig. 5A–D). These findings suggest that these genes may play crucial roles in the pathogenesis or progression of aSAH and could potentially serve as biomarkers or therapeutic targets for this condition.

3.5. Survival analysis of key genes

To evaluate the predictive performance of the model in predicting aSAH, we conducted receiver operating characteristic (ROC) curve analysis. (area under the model's ROC curve = 0.908), and a nomogram was employed to predict the occurrence of aSAH (Fig. 6 A, B). The AUC for both the ARHGAP26 and SLMAP genes exceeded 0.8, suggesting that they possess considerable diagnostic potential for aSAH (Fig. 6C).

3.6. Immune infiltration score and correlation analysis

The SSGSEA enrichment scores of various immune cell subpopulations, associated functions, and pathways were measured in individuals with ruptured and unruptured intracranial aneurysms. The

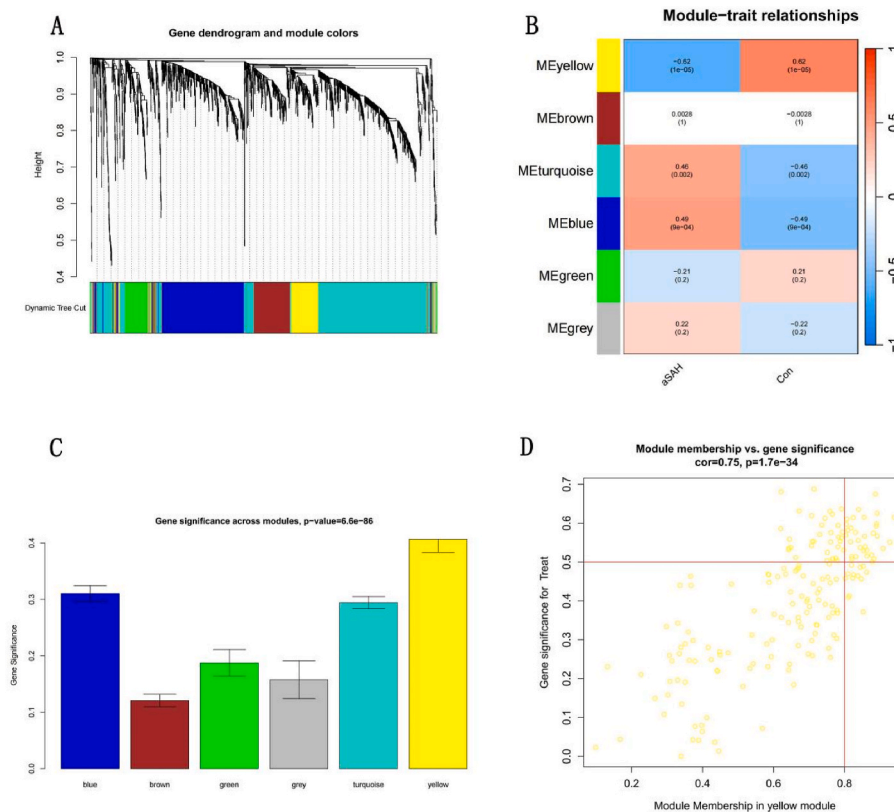


Fig. 2. Weighted correlation network analysis (WGCNA) of samples. (A) Cluster dendrogram among modules. (B) Module-trait relationships. The darker the module color, the more significant their relationship. (C) Distribution of average gene significance and errors in the modules associated with aSAH status. (D) A scatter plot of the GS for aSAH versus the MM in the yellow module. (For interpretation of the references to color in this figure legend, the reader is referred to the Web version of this article.)

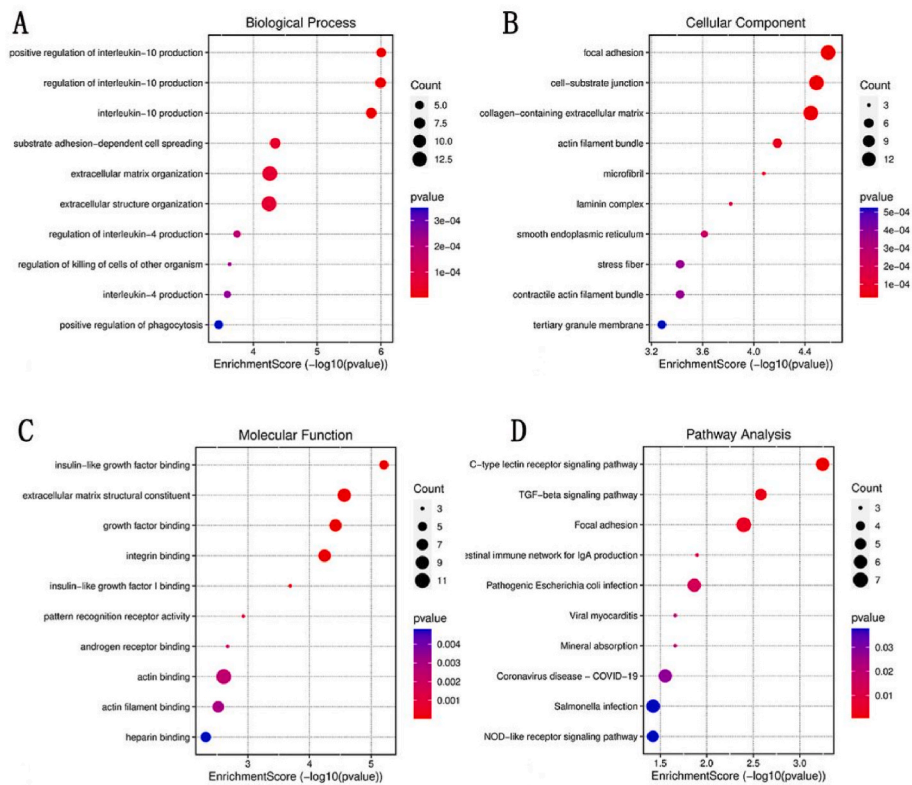


Fig. 3. Functional enrichment analysis of aSAH-related genes. A. Enrichment analysis of GO-biological processes (GO-BP). B. Enrichment analysis of GO-cellular component (GO-CC). C. Enrichment analysis of GO-molecular function (GO-MF). D. KEGG pathway analysis.

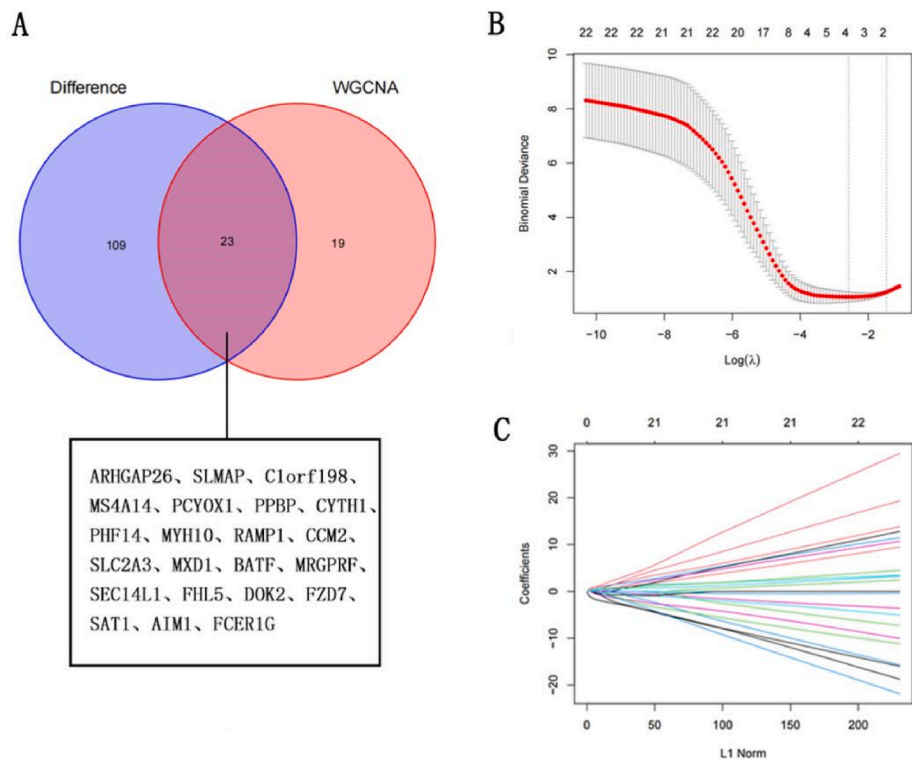


Fig. 4. Screening of key genes. A Venn diagram. B The logistic regression model for the training set was conducted to identify an optimum linear combination in predicting responsiveness. C Cross-Validation Fit Plot.

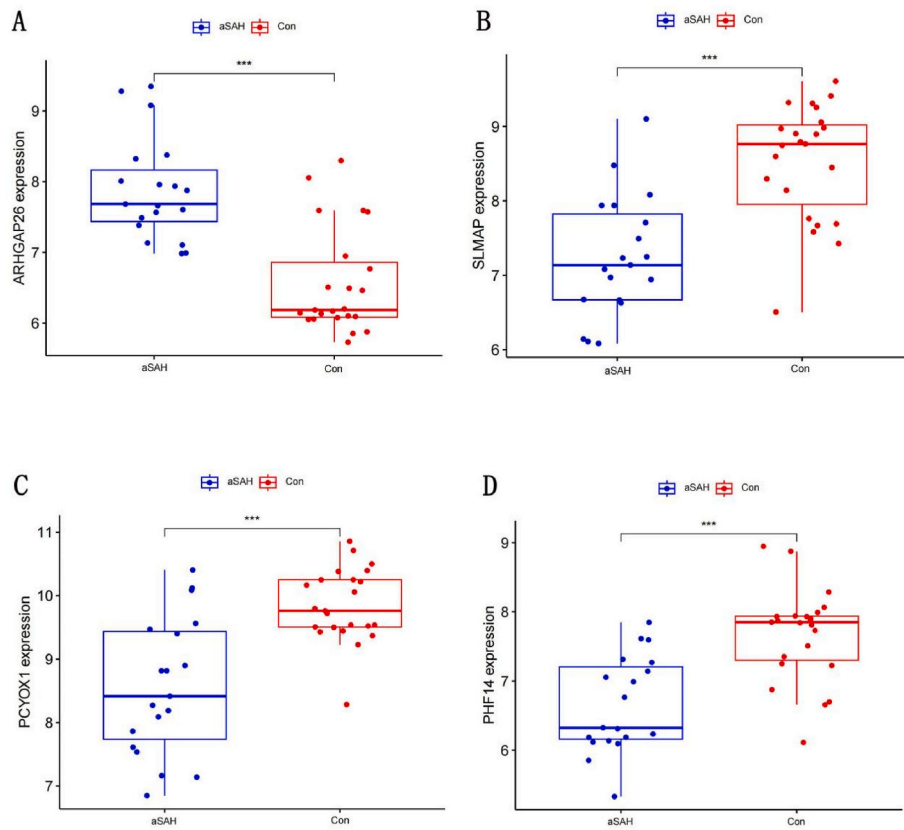


Fig. 5. Expression of differential genes in aSAH and control groups. ns $P > 0.05$; * $P \leq 0.05$; ** $P \leq 0.01$; *** $P \leq 0.0001$.

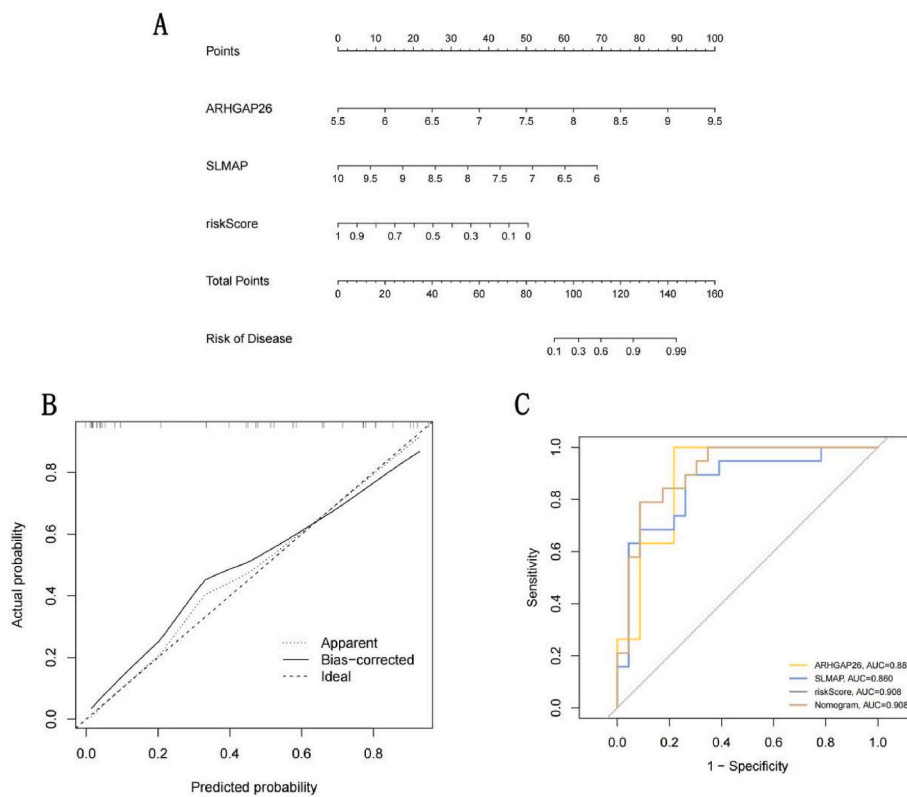


Fig. 6. Survival analysis of key genes A. Nomogram predicting for aSAH patients; B. Calibration curves for nomogram predicted aSAH patients; C. ROC curve analysis show highest AUC value was seen for the nomogram mode.

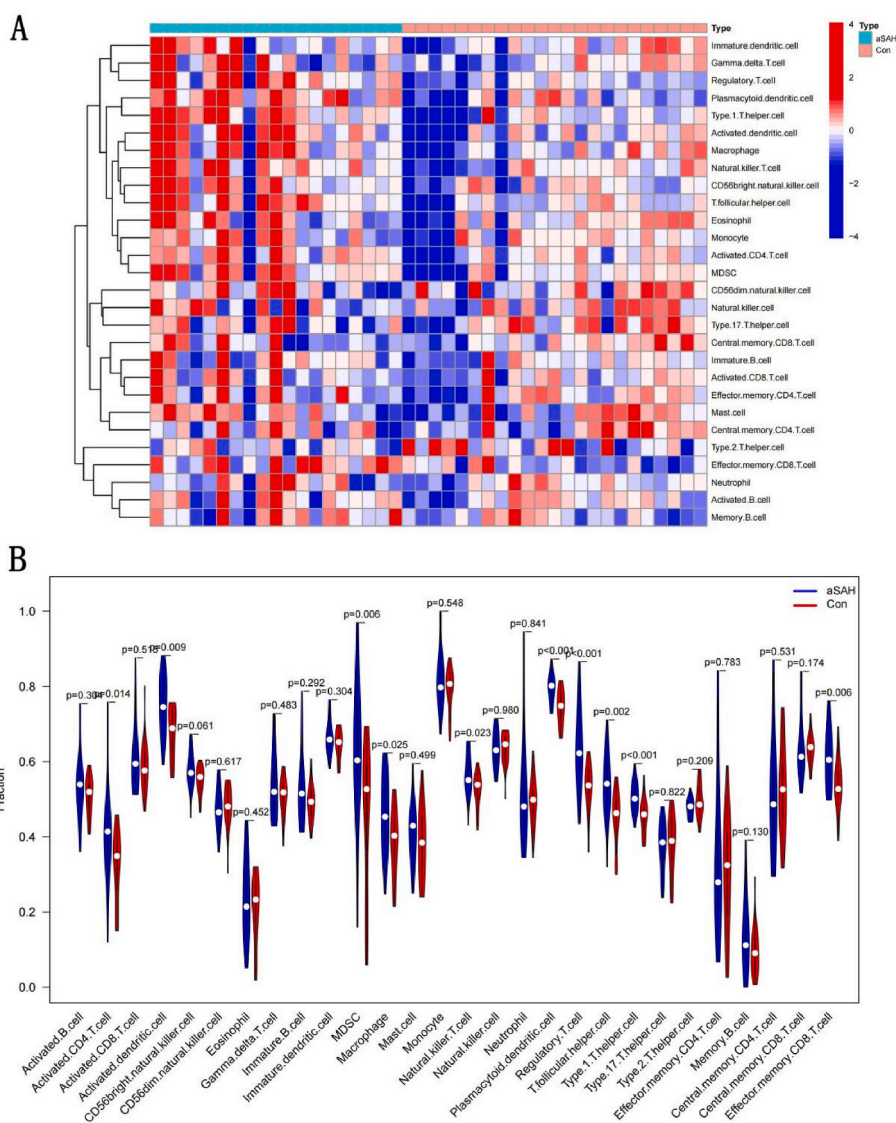


Fig. 7. Immune correlation analysis A. Landscape evaluation of 29 types of immune signatures in two subgroups of aSAH samples. B. The Violin diagram showed the difference of immune infiltration between aSAH and Con groups. The aSAH group was marked as blue, and the Con group was marked as red ($p < 0.05$ was regarded as statistical significance). (For interpretation of the references to color in this figure legend, the reader is referred to the Web version of this article.)

correlation heatmap depicting the relationships among the 29 types of immune signatures demonstrated significant positive correlations between Type 1 T helper cell (Th1 cell), Activated dendritic cell (DC), Macrophage cell and etc (Fig. 7A). The abundance of immune cells and immune functions in each sample is shown in a heatmap (Fig. 7B).

4. Discussion

The occurrence of a ruptured intracranial aneurysm resulting in SAH is a prevalent cerebrovascular ailment, necessitating surgical intervention as the sole viable treatment approach. However, it is worth noting that a significant number of patients frequently experience profound neurological complications that have a substantial detrimental effect on their overall quality of life [9]. The present diagnostic modality employed for SAH is CT scan, which exhibits a sensitivity ranging from approximately 93%–100 % during the initial 6 h following the onset of clinical symptoms. DSA is considered the preferred diagnostic method for determining the cause and planning the surgical approach for SAH. However, CT angiography (CTA) can serve as a viable alternative for monitoring purposes, with a combined sensitivity of 97 % and specificity of 91 % [10,11]. SAH exhibits complex pathological and physiological

processes. Previous studies have identified various potential mechanisms underlying SAH, including neuroinflammation, microthrombus formation, cortical spreading depolarization, disruption of the blood-brain barrier, microvascular dysfunction, sympathetic-adrenal activation, and dysfunction of endothelial cells [12,13]. This study aimed to identify the characteristic genes associated with SAH, investigate their biological functions and expression levels, construct ROC curves for these genes, and perform immune cell infiltration analysis to contribute to the prediction and treatment of aSAH.

The present study involved the integration of two datasets, namely GSE13353 and GSE54083, for the purpose of identifying genes that exhibit differential expression. Through this analysis, a total of 132 genes were identified as differentially expressed, comprising 63 genes that were up-regulated and 69 genes that were down-regulated. We generated weighted gene co-expression networks for both ruptured and unruptured intracranial aneurysms, resulting in the identification of six distinct gene modules. Through the process of intersecting the genes, a total of 23 genes were identified. Subsequent LASSO regression analysis has identified ARHGAP26, SLMAP, PCYOX1, and PHF14 as key genes associated with ruptured intracranial aneurysms that result in subarachnoid hemorrhage. This study employed single-factor and multiple-

factor logistic regression analysis to ascertain the significance of ARHGAP26 and SLMAP as pivotal genes in the prediction of aSAH. The predictive value of ARHGAP26 for subarachnoid hemorrhage was found to be statistically significant (AUC: 0.888, 95 % CI: 0.767–0.975). The ARHGAP26 gene, alternatively referred to as the GRAF gene, is responsible for the synthesis of a protein that functions as a modulator of small GTP-binding proteins within the Rho family and can bind to protein tyrosine kinases [14,15]. Previous studies have demonstrated that the ARHGAP26 gene exerts significant regulatory influence on the advancement of various diseases, including leukemia, brain tumors, gastric cancer, and ovarian cancer [14,16–19]. Additionally, this gene has been implicated in the development of progressive muscle degeneration, intellectual disability, and neuro-psychiatric disorders. According to a study conducted by Kesheng Wang [14], it was discovered that the ARHGAP26 gene has a significant regulatory function in the progression of Alzheimer's disease, as well as cardiovascular and cerebrovascular diseases. The sarcolemmal membrane-associated protein (SLMAP) is a member of the tail-anchored membrane protein family and is generally downregulated in individuals diagnosed with dilated cardiomyopathy and heart failure [20]. The present study observed a decrease in SLMAP expression in individuals diagnosed with SAH resulting from ruptured intracranial aneurysms. Furthermore, it was determined that SLMAP expression exhibited some predictive capability for the occurrence of aSAH (AUC: 0.860, 95%CI: 0.732–0.961). The line chart depicted a cumulative score of 160 points. Notably, when the cumulative score surpassed 130 points, the predictive value for the risk of aSAH exceeded 90 %. This value was found to be significantly higher than the AUC values observed in other models utilizing single indicators. The findings of this study indicate that the developed aSAH risk prediction model exhibited a high level of accuracy and demonstrated significant clinical applicability.

Several studies have demonstrated that immune and inflammatory responses are significant factors in the pathogenesis of SAH resulting from ruptured intracranial aneurysms [21]. When an intracranial aneurysm ruptures, blood accumulates in the subarachnoid space [22]. Subsequently, neutrophils and macrophages phagocytose the byproducts resulting from the degradation of red blood cells, which triggers a cascade of inflammatory response cells at different levels. The enrichment analysis of GO and KEGG pathways conducted on the differentially expressed genes in the context of aSAH revealed that the primary biological processes involved are cell cycle regulation, cell proliferation, cell adhesion, and promoter binding. Numerous studies have demonstrated that intracranial aneurysm is primarily attributed to apoptosis and proliferation of endothelial cells and smooth muscle cells, along with immune cell infiltration [23,24]. The initiation of innate immunity is facilitated by immune receptors. Recent research has revealed that the C-type lectin receptor (Mincle) induced by microglia can sense the subunit SAP13 of the histone deacetylase of dead cells by binding. Following stimulation, the activation of Mincle and its downstream molecule spleen tyrosine kinase (Syk) can initiate signaling pathways that lead to the production of inflammatory cytokines, consequently facilitating the recruitment of neutrophils [25–27]. In their study, Xie et al. [28], discovered that microglia macrophages trigger the innate immune response of microglia following SAH through the activation of the C-type lectin receptor known as Mincle. This process was identified as a crucial early event in the development of brain injury subsequent to SAH. The present study has identified that the signaling pathway mediated by C-type lectin receptors plays a significant role in the pathogenesis of aSAH, as evidenced by the results of enrichment analysis. Additionally, the immune system plays a significant role in the initiation and progression of acute inflammation, which can be triggered by microbial infection or tissue damage. Moreover, our investigation revealed that B cells, neutrophils, and CD8⁺ T lymphocytes constitute the principal immune cell types in the context of ssGSEA.

To conclude, the present study has successfully identified two crucial genes associated with aSAH, specifically ARHGAP26 and SLMAP.

Furthermore, our findings suggest that these genes potentially modulate immune cell infiltration as a mechanism of action. The present study, thus, offers novel perspectives that can inform future investigations into the pathogenesis of aSAH. Nevertheless, we acknowledge the limitations of our study, as it relied on a secondary analysis of previously published data. Although our findings offer valuable insights, the reliability and robustness of the present study could be enhanced through additional validation using *in vivo* and *in vitro* experiments. Such experimental validation would bolster the confidence in our results and provide a more comprehensive elucidation of the underlying biological mechanisms.

Declaration of competing interest

No conflicts of interest to declare.

Data availability

Data will be made available on request.

References

- [1] Yi Dong, Zhen-Ni Guo, Li Qi, et al., Chinese Stroke Association guidelines for clinical management of cerebrovascular disorders: executive summary and 2019 update of clinical management of spontaneous subarachnoid haemorrhage, *Stroke Vascular Neurol.* 4 (4) (2019) 176–181.
- [2] T. Lawton Michael, G Edward Vates, Subarachnoid hemorrhage, *N. Engl. J. Med.* 377 (3) (2017) 257–266.
- [3] Macdonald R. Loch, A. Schweizer Tom, Spontaneous subarachnoid haemorrhage, *Lancet (N. Am. Ed.)* 389 (10069) (2017) 655–666.
- [4] A. Rava Ryan, E. Seymour Samantha, E. LaQue Meredith, et al., Assessment of an Artificial Intelligence Algorithm for Detection of Intracranial Hemorrhage vol. 150, *World Neurosurgery*, 2021, pp. e209–e217.
- [5] Hiroharu Kataoka, Takanobu Yagi, Ikedo Taichi, et al., Hemodynamic and histopathological changes in the early phase of the development of an intracranial aneurysm, *Neurol. Med.-Chir.* 60 (7) (2020) 319–328.
- [6] M.I. Kurki, S.K. Häkkinen, J. Frösen, R. Tulamo, et al., Upregulated signaling pathways in ruptured human saccular intracranial aneurysm wall: an emerging regulative role of Toll-like receptor signaling and nuclear factor- κ B, hypoxia-inducible factor-1A, and ETS transcription factors, *Neurosurgery* 68 (6) (2011 Jun) 1667–1675, discussion 1675–6.
- [7] H. Nakaoka, A. Tajima, T. Yoneyama, K. Hosomichi, et al., Gene expression profiling reveals distinct molecular signatures associated with the rupture of intracranial aneurysm, *Stroke* 45 (8) (2014 Aug) 2239–2245.
- [8] J. Pera, M. Korostynski, S. Golda, M. Piechota, et al., Gene expression profiling of blood in ruptured intracranial aneurysms: in search of biomarkers, *J. Cerebr. Blood Flow Metabol.* 33 (7) (2013 Jul) 1025–1031.
- [9] J. Benson Melissa, Manzanero Silvia, Borges Karin, Complex alterations in microglial M1/M2 markers during the development of epilepsy in two mouse models, *Epilepsia* 56 (6) (2015) 895–905.
- [10] Hou Sherry Hsiang-Yi, Subarachnoid Hemorrhage. Continuum (Minneapolis, Minn.), 2021, pp. 1201–1245, 27 (5).
- [11] N. Neifert Sean, K. Chapman Emily, L. Martini Michael, et al., Aneurysmal subarachnoid hemorrhage: the last decade, *Translat. Stroke Res.* 12 (3) (2021) 428–446.
- [12] L. Osgood Marcey, Aneurysmal subarachnoid hemorrhage: review of the pathophysiology and management strategies, *Curr. Neurol. Neurosci. Rep.* 21 (9) (2021) 50.
- [13] R. Geraghty Joseph, L. Davis Joseph, D. Testai Fernando, Neuroinflammation and microvascular dysfunction after experimental subarachnoid hemorrhage: emerging components of early brain injury related to outcome, *Neurocritical Care* 31 (2) (2019) 373–389.
- [14] Kesheng Wang, Yongke Lu, F. Morrow Deana, et al., Associations of ARHGAP26 polymorphisms with Alzheimer's disease and cardiovascular disease, *J. Mol. Neurosci.* 72 (5) (2022) 1085–1097.
- [15] Emma Monte, M. Vondriska Thomas, Epigenomes: the missing heritability in human cardiovascular disease? *Proteomics Clin. Appl.* 8 (7–8) (2014) 480–487.
- [16] L.V. Wangxia, Fang Yang, Yongjun Liu, et al., Circular RNA ARHGAP26 is over-expressed and its downregulation inhibits cell proliferation and promotes cell apoptosis in gastric cancer cells, *Saudi J. Gastroenterol.* 25 (2) (2019) 119–125.
- [17] Xuri Chen, Shaoyun Chen, Li Yao, et al., SMURF1-mediated ubiquitination of ARHGAP26 promotes ovarian cancer cell invasion and migration, *Exp. Mol. Med.* 51 (4) (2019) 1–12.
- [18] Minghui Li, Lincui Ye, Xiuxia Ye, et al., Hypoxia-induced ARHGAP26 deficiency inhibits the proliferation and migration of human ductus arteriosus smooth muscle cell through activating RhoA-ROCK-PTEN pathway, *J. Cell. Biochem.* 120 (6) (2019) 10106–10117.

- [19] Dahm Liane, Christoph Ott, Johann Steiner, et al., Seroprevalence of autoantibodies against brain antigens in health and disease, *Ann. Neurol.* 76 (1) (2014) 82–94.
- [20] Nader Moni, Alsolme Ebtehal, Alotaibi Shahd, et al., SLMAP-3 is downregulated in human dilated ventricles and its overexpression promotes cardiomyocyte response to adrenergic stimuli by increasing intracellular calcium, *Can. J. Physiol. Pharmacol.* 97 (7) (2019) 623–630.
- [21] Kleinloog Rachel, H. Verweij Bon, van der Vlies Pieter, et al., RNA sequencing analysis of intracranial aneurysm walls reveals involvement of lysosomes and immunoglobulins in rupture, *Stroke* 47 (5) (2016) 1286–1293.
- [22] P. Lucke-Wold Brandon, F. Logsdon Aric, Manoranjan Branavan, et al., Aneurysmal subarachnoid hemorrhage and neuroinflammation: a comprehensive review, *Int. J. Mol. Sci.* 17 (4) (2016) 497.
- [23] S. Turjman Alexis, Turjman Francis, R. Edelman Elazer, Role of fluid dynamics and inflammation in intracranial aneurysm formation, *Circulation* 129 (3) (2014) 373–382.
- [24] Ming Zhao, Longbiao Xu, Hui Qian, Bioinformatics analysis of microRNA profiles and identification of microRNA-mRNA network and biological markers in intracranial aneurysm, *Medicine* 99 (31) (2020), e21186.
- [25] Kooijman Elke, H. Nijboer Cora, T.J. van Velthoven Cindy, et al., Long-term functional consequences and ongoing cerebral inflammation after subarachnoid hemorrhage in the rat, *PLoS One* 9 (6) (2014), e90584.
- [26] Juan Carlos de Rivero Vaccari, J. Brand Frank, F. Berti Aldo, et al., Mincle signaling in the innate immune response after traumatic brain injury, *J. Neurotrauma* 32 (4) (2015) 228–236.
- [27] Yue He, Xu Liang, Li Bo, et al., Macrophage-Inducible C-type lectin/spleen tyrosine kinase signaling pathway contributes to neuroinflammation after subarachnoid hemorrhage in rats, *Stroke* 46 (8) (2015) 2277–2286.
- [28] Yi Xie, Hongquan Guo, Liumin Wang, et al., Human albumin attenuates excessive innate immunity via inhibition of microglial Mincle/Syk signaling in subarachnoid hemorrhage, *Brain Behav. Immun.* 60 (2017) 346–360.